Contrib. Plasma Phys. **49**, No. 7-8, 570 – 576 (2009) / **DOI** 10.1002/ctpp.200910057

Experimental Study of Hard X-Ray Production at Sub-Relativistic Intensities: Effect of Polarization and Nanosecond Pre-Pulse

V. V. Bolshakov[1], **A.A. Vorobiev**[1,2], **R.V. Volkov**[1], and **A.B. Savel'ev**[*1]

[1] International Laser Center & Faculty of Physics, Lomonosov Moscow State University Leninskie gory, 119991, Moscow, Russia

[2] Prokhorov General Physics Institute of Russian Academy of Sciences Vavilova str.38, 119991, Moscow, Russia

Received 15 April 2009, accepted 30 June 2009
Published online 08 October 2009

Key words X-ray lasers.
PACS 42.55.Vc

?

1 Introduction

For the plasma formed under interaction of femtosecond laser radiation with the surface of a target electron velocity distribution has fundamentally non-maxwellian shape: besides thermal electrons, taking their origin from classical collisional mechanisms, hot electron component is formed. In particular such important effects as generation of hard X-rays with high spectral intensity and small pulse duration, protons and multicharged ions acceleration to high energies, nuclear reactions in plasma and so on, are closely linked with hot electrons.

Generation of the hot electron component is related to additional, non-collisional mechanisms of electrons heating; its mean energy exceeds mean energy of thermal component by 1-2 orders [1]. Orientation of linear polarization of radiation with respect to plasma's electron density gradient plays important role at moderate intensities (10^{15}-10^{17}W/cm^2), because all the basic mechanisms (anomalous skin-effect [2, 3], resonant absorption [4–6] and vacuum heating [6, 7]) do not work for s-polarized radiation and hot electrons are not generated.

With intensities higher than relativistic threshold (10^{18} W/cm^2), most important role in electrons acceleration play such phenomena as ponderomotive potential [8], $[v \times B]$ component of the Lorentz force [9, 10] and wake-field acceleration [11, 12]. In particular, above-mentioned mechanisms are not sensitive to linear polarization orientation of laser radiation, but differ depending linear or circular polarization of laser radiation is used [13].

Intermediate range of subrelativistic intensities, when impact from all the mentioned mechanisms of hot electron component generation is possible, is investigated in much less details. Generation of hot electrons with s-polarized radiation becomes possible in this range, while hot electrons energy distribution may contain several components due to effect of different physical mechanisms.

Starting with moderate intensities, important role in interaction of femtosecond laser pulse with supercritical dense plasma plays presence of a pre-pulse, which intensity may exceed target's surface breakdown threshold ($\sim 10^{11}$-10^{13} W/cm^2 depending on the target material). In such conditions main pulse interacts with diffused plasma-vacuum boundary and spatial scale of electron density essentially defines main mechanism of hot electrons generation. With laser radiation intensity increase pre-pulse's influence increases as well.

In this work we present results of hot electrons generation study during interaction of femtosecond laser radiation with subrelativistic intensity (from 10^{15} to 210^{17} W/cm^2), having different linear polarization and nanosecond contrast, with surfaces of transparent (quartz glass) and absorbing (silicon) targets. Also, it is experimentally shown, that irradiating a bulk target with pair of femtosecond laser pulses (delay between pulses equal to 13 ns),

* Corresponding author: e-mail: fantik413@gmail.com

forming radiation with contrast 100-500 and intensity $\sim 10^{18}$ W/cm^2, results in prominent growth of hot electrons mean energy in comparison with the high contrast case $\sim 10^6$.

2 Experimental setup and methods

All our experiments were carried out using radiation of femtosecond Ti:Sa laser system of ILC MSU [14] (pulse duration 50 ± 5 fs, peak power 0,3 TW, wavelength 800 nm). For laser system being used, contrast on nanosecond time scale is defined by the pre-pulse, advancing the main pulse by 13 ns and having 4×10^6 times less amplitude, and on picosecond time scale by series of pre-pulses, maximal of which comes 7 ps ahead the main pulse and has 5×10^4 times less amplitude. Relative level of the amplified spontaneous radiation on picosecond time scale does not exceed 10^5. Beam quality factor equals to $M^2=1.8\pm0.3$.

Orientation of linear polarization during experiments was changed by means of half-wave plate. Nanosecond contrast control was realized by turning off additional Pockels cell, installed between regenerative and multipass amplifiers of the laser system, which resulted in contrast reduction up to 10^3. Further contrast degradation to $\sim$40 was realized by misalignment of Pockels cell polarizers in the regenerative amplifier. With misaligned Pockels cell in this amplifier and the additional Pockels cell turned on, contrast was 2x10^3.

In the first series of experiments we have used silicon (Si) and quartz glass (SiO_2) targets. The aberration-free objective (focal length $\sim$6 cm) focused laser beam into 4 mkm diameter spot. Peak intensity in experiments was 2x10^{17} W/cm^2 with 2mJ pulse energy. Plain solid target was oriented at 45° angle with respect to the laser beam. Target was fixed on 2D step motor translator in the vacuum chamber with residual pressure about 10^{-2} torr. Target was shifted in horizontal dimension with constant velocity during the experiment, while remaining in the focal plane.

In order to estimate hot electrons' mean energy, measurements of X-rays yield into different spectral ranges were carried out. The low energy cut-off was determined by the thickness of the filter, placed in front of the detector, while the high energy threshold was constant and equal to 100 keV. Dependence of X-rays yield from the filters' low-pass edge energy was fitted by decay exponential function. Exponent index's value was used as an estimate of hot electrons' mean energy later on.

In the second series of experiments plain thick plate of tungsten was used as a target. The target, as well as the whole optical focusing scheme, was placed into the vacuum chamber with 10^{-2} torr residual pressure. Laser radiation was focused on the target's surface by off-axes parabolic mirror (F/D$\sim$5) into a 3.5 mkm diameter spot, containing 55% of pulse's energy.

Hard X-rays from laser plasma were registered in experiments. Single-quantum mode of photon registration was realized by varying the distance between plasma source and detector, as well as by using of different combinations of apertures and filters. Mean probability of single quantum registration during one laser pulse was equal to 0.1. Distribution of X-rays quanta was built upon 5000-10000 laser shots.

3 Experiments at 10^{17}W/cm^2 and below

We have investigated hot electrons' mean energy dependence on the orientation of linear polarization, as well as on the nanosecond contrast value (intensity 2x10^{17} W/cm^2 and 10 Hz laser pulses repetition rate). Our findings, summarized in tab. 1, show that hot electrons are effectively generated even upon effect of s-polarized laser radiation. Moreover, difference between X-rays yield and hot electrons mean energy for s- and p- polarization is very small.

As already mentioned, at moderate intensities efficient generation of hot electrons on flat plasma-vacuum bound is possible for p-polarized radiation only, because it has field component, parallel with electron density gradient. Hot electrons generation by s-polarized radiation in this interaction mode is possible only due to plasma-vacuum interface (or a critical density surface) distortion. Less difference between s- and p- polarized radiation cases also appears in relativistic interaction mode.

Formation of the curved boundary in our experiments could be possible because of spatial intersection of the interaction regions of consequent laser pulses at 10 Hz repetition rate. In 10 Hz mode radiation interacts with target's surface, partially modified by the previous laser pulse, while in 1 Hz mode target has enough time to move away and, as a result, surface is non-distorted when the next laser pulse comes.

Table 1 Hot electrons' mean energy (in keV) upon effect of laser radiation on Si and SiO_2 targets

Target		Si		SiO_2	
Contrast		4×10^6	10^2	4×10^6	10^2
polarization	Rep.rate, Hz				
p	1	18,2±1,1	16,8±1,0	15,3±0,9	18,1±1,2
p	10	14,2±0,9	11,5±0,8	13,1±0,8	14,7±0,9
s	1	16,0±0,9	14,3±0,9	12,2±0,8	15,7±0,9
s	10	11,4±0,8	10,6±0,8	10,4±0,7	11,9±0,8

Mean energies of hot electrons, obtained at two repetition rates of laser pulses for Si and SiO_2 targets at intensity 2x10^{17} W/cm^2, are also presented in the table 1. One can see that mean energies of hot electrons differ weakly for p- and s- polarized radiation at 1 and 10 Hz repetition rates for both targets. Hence, weak difference in mean energies of hot electrons for the two used polarizations of laser radiation at intensity 2x10^{17} W/cm^2 is not connected with plasma-vacuum boundary distortion.

It is necessary to note increase in the hot electrons' mean energy at 1 Hz interaction regime regardless parameters of laser radiation. We have obtained similar results at lower intensity as well. Observed decrease of hot electrons' mean energy during multiple effects on target contradicts known fact that hard X-rays yield and hot electrons' mean energy increase upon effect of femtosecond laser radiation at the same surface area [15, 16]. In particular, this contradiction may come from continuous displacement of the target in our experiments.

An alternative explanation of weak difference in hard X-rays yield and hot electrons' mean energy for p- and s-polarized laser radiation in our experiments may be connected with mechanisms of hot electrons generation, substantial at relativistic intensities. At intensity $\sim10^{17}$ W/cm^2 ponderomotive potential becomes as large as $T_p \sim$ 23 keV, which can bring to generation of sufficient amount of hot electrons with energies about T_p, moreover, this effect does not depend on orientation of laser pulse's linear polarization.

To clear up our guess, the experiment on studying dependence of plasma parameters upon laser radiation intensity was carried out with nanosecond contrast 4x10^6 and 10 Hz repetition rate using quartz glass target. Intensity on the target was decreased by displacing focusing objective with respect to the target from precise focus position. Intensity was estimated using classic Gaussian beam formulas [17], taking into account beam quality parameter M^2.

Dependence of hot electrons mean energy on laser radiation intensity for two polarizations is presented in fig.1. In $10^{15} - 10^{16}$W/cm^2 intensity range we observed prominent excess of the hot electrons mean energy, obtained with the p-polarized laser radiation, over the mean energy, obtained with the s-polarized radiation, which fits theoretical concepts and experimental data [[1]]. For the p-polarized radiation and within the mentioned intensity range the hot electrons mean energy grows with intensity as

$$E_{el}[keV] \approx (4,1 \pm 0.1) \cdot \left(I_{16} \cdot \lambda_\mu^2\right)^{0.30\pm0.02}$$

Here I_{16} is intensity, normalized to 10^{16} W/cm^2, λ_μ - wavelength in micrometers. This dependence lies in reasonable agreement with known relation for hot electrons mean energy, formed due to resonant absorption of laser radiation [[5]]:

$$E_{el}[keV] \approx 14 \cdot \left(I_{16} \cdot \lambda_\mu^2\right)^{0.33} \cdot T_c^{0.33}\,. \tag{1}$$

Here T_c is thermal electrons temperature, $T_c \sim 0.3 - 0.5$ keV.

With intensities around 10^{16} W/cm^2 one can notice clear bend in fig.1 graphs plotted for the p-polarized case. The bend in dependence of the hot electrons mean energy on laser pulse's intensity may take its origin from the spatial scale change in the expanding pre-plasma, which is formed by the picosecond pre-pulse, because the pre-pulse's intensity grows as the main pulse's intensity grows. Besides, the resonant absorption at sub-relativistic intensities may have much more complex nature, while its efficiency may decrease [[18]].

Hard X-rays from plasma were registered at intensities more than 2x10^{16} W/cm^2 for s-polarized laser radiation (see fig. 1). This intensity lies in rough agreement with surface breakdown threshold by picosecond pre-pulse with 2x10^3 contrast [19], [20]. As already mentioned, hot electrons generation by s-polarized laser radiation is possible

due to relativistic effects. Generally, these mechanisms work effectively on distorted plasma-vacuum boundary, and this fact explains generation of hot electrons only at intensities more than threshold of surface breakdown by a pre-pulse. Particularly, as shown in [[21]], starting with intensities about 10^{17} W/cm^2, hot electron component expansion is co-directed with reflected laser beam, rather than laser radiation polarization. This also demonstrates important role of relativistic mechanisms in hot electrons acceleration at specified intensity value. Hot electrons mean energies ratio for s- and p- polarized laser radiation dependence on laser pulse's intensity is also depicted in fig. 1. One can see that the ratio tends to 1 with intensities approaching 10^{17} W/cm^2.

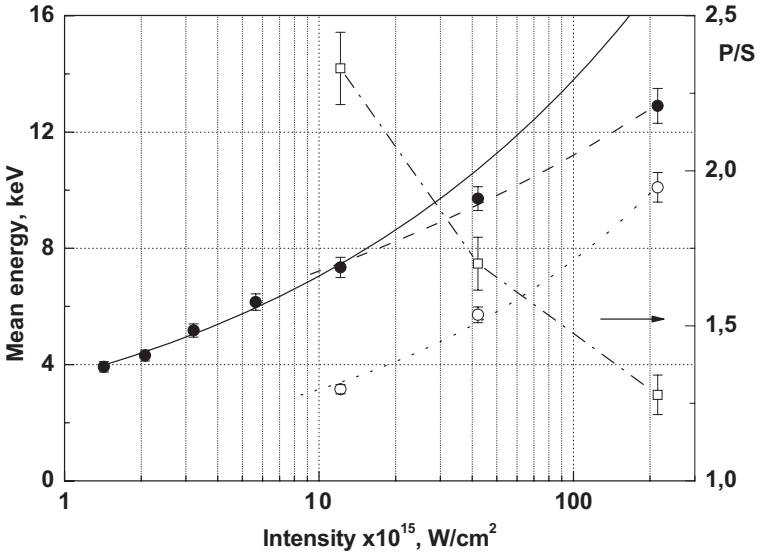

Fig. 1 Mean energy of hot electrons for p-(experiment – •, fitting – solid and dashed line) and s-(experiment – ○, fitting – dotted line) polarization, as well as hot electrons mean energies ratio P/S, obtained for p- and s-polarization (□ and dash-dotted line) for SiO_2 target, depending on laser radiation intensity.

As observed in the obtained experimental data, pre-plasma, which is formed by the pre-pulse, plays important role in the interaction of femtosecond laser pulse with plasma, starting with intensities as large as 10^{17} W/cm^2. The picosecond pre-pulse played the most important role in plasma generation in discussed experiments, with its relative amplitude depends on laser system parameters and remains constant. At the same time, our laser system allows one to control amplitude of a pre-pulse, which is advancing the main pulse by 13 ns.

In the view of the aforesaid, we have carried out measurements of hot electrons mean energies dependencies on nanosecond pre-pulse amplitude; results are partially presented in tab. 1. The main feature is monotonic growth of hot electrons mean energy with laser radiation contrast increase for Si target. On the contrary, for SiO_2 target the hot electrons mean energy monotone decreases with laser radiation contrast increase. In both cases switching to s-polarization from p-polarization slightly affects the mean energy value.

4 Experiments above 10^{18}W/cm^2

In individual series of experiments the hot electrons mean energy dependence on the nanosecond pre-pulse amplitude at intensities 10^{17} – 10^{18} W/cm^2 was measured. Typical spectrum of X-radiation, built upon 7000 laser pulses at best laser radiation contrast and 15 mJ pulse energy, is presented in fig. 2.

The spectrum contains two well-distinguished components with different mean energies (slopes). Estimated mean energy for quanta with energies less than 200 keV is T_1 $\sim$41$\pm$3 keV, for quanta with energies higher than 200 keV – T_2 $\sim$134$\pm$9 keV. Thus, in our experimental conditions at least 2 components are formed in electron velocity distribution (excluding thermal electron component). Generation of electrons, having lesser mean energy, may be related to the resonant absorption in plasma critical density region. According to [5] in our experimental conditions the mean energy of hot electrons, generated due to the resonant absorption and having energies less than 200 keV, may be estimated asfrom (1) as a 44 – 55 keV when I$\sim$2x10^{18} W/cm^2. Generation of

the electron component, having higher mean energy, may be related to resonant absorption [22], ponderomotive electron acceleration [8] and [$\mathbf{v}\times\mathbf{B}$] heating [10].

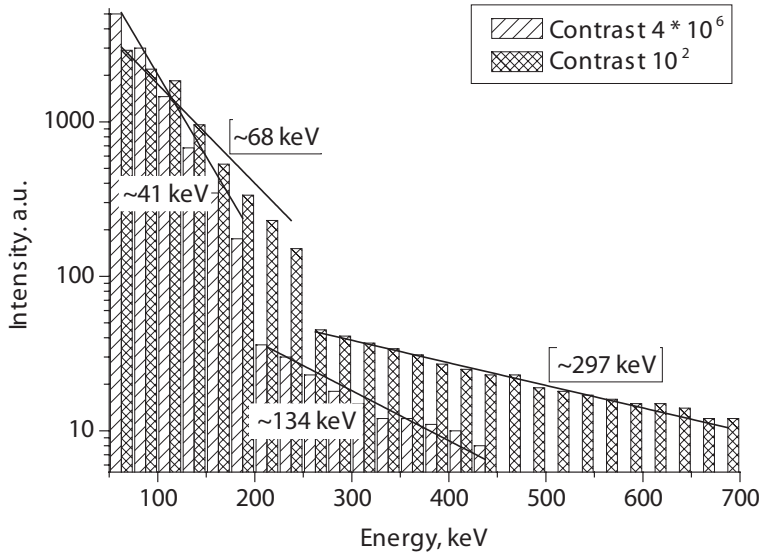

Fig. 2 Typical spectrum of X-radiation at 15 mJ laser pulse energy.

The X-ray radiation spectrum remarkably changes at lower contrast of 100 (see fig. 2). In particular, X-rays quanta with energies up to 2 MeV were registered. The mean energies of both electron components increased and became $T_2 \sim 297\pm9$ keV, $T_1 \sim 68\pm7$ keV.

Measurement of electrons mean energy T_2 dependence on laser radiation intensity was carried out by changing laser pulse's energy via polarization attenuator, being installed between the multi-pass amplifier and the compressor. Experimental results are presented in fig. 3 for 500 and $4x10^6$ contrast values.

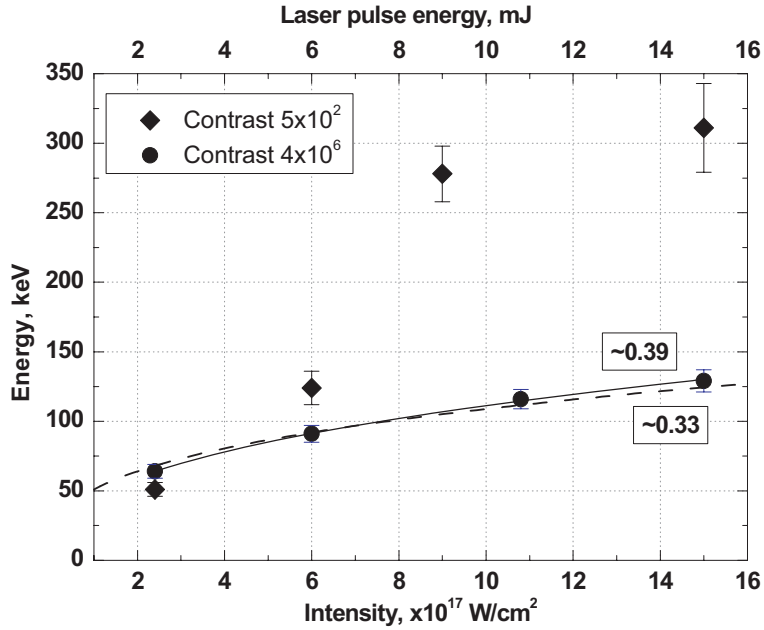

Fig. 3 Electrons mean energy dependence on laser radiation intensity.

Fitting of the obtained dependence at maximal laser radiation contrast by power function gives us $T_2 \sim (73 \pm 2) \cdot (I_{17}\lambda^2)^{0.39\pm0.02}$ keV. Estimated fitting is inconsistent with resonant absorption formula $T_2 \propto (I\lambda^2)^{0.33}$ and ponderomotive acceleration formula $T_2 \propto \left[\left(1 + {I\lambda^2}/{I_r}\right)^{0.5} - 1\right]$. At the same time estimated at maximal intensity value $T_2 \sim 134 \pm 9$ keV is in reasonable agreement with calculation, based on ponderomotive potential value at intensity 1.5x10^{18} W/cm^2. Difference between our fitting and well-known formulas may be partially related to the fact that pre-pulse's intensity grows as pulse's energy grows, while the contrast is fixed.

At the contrast of 500 the observed dependence is remarkably different. At intensity $\sim$ 2x10^{17} W/cm^2 the mean energy of electrons weakly depends on the contrast and amounts to 50 keV. Intensity increase while leaving the contrast fixed results in fast, threshold-like growth of electrons' mean energy, which becomes as large as 270 keV at intensity $\sim 10^{18}$ W/cm^2. With further increase of the laser radiation intensity electrons' mean energy growth rate falls down and mean energy becomes $\sim$300 keV at intensity 1.5x10^{18} W/cm^2.

It should be denoted that the mean energy of hot electrons in the first series of experiments at intensities $\sim 10^{17}$ W/cm^2 was found to be $\sim$ 15 keV, while in the second series of experiments – $\sim$ 50 keV. Seemingly, this difference is connected with the fact, that there are actually several hot electron components in plasma, and using different measurement techniques we assessed different components' mean energies.

5 Discussion and conclusions

Thus, comparative investigation of hot electrons' generation at intensities up to 2x10^{17} W/cm^2 using transparent target (quartz glass) and solid target (silicon) showed, that relativistic effects play noticeable role even at intensities one order less than the relativistic one. In particular, they lead to effective generation of hot electrons by s-polarized laser radiation, and mean energy of such electrons is almost equal to the similar value for the p-polarized radiation.

If the pre-pulse exists in temporal structure of laser radiation and has nanosecond delay and high enough amplitude (0.002-0.01 to that of the main pulse), dependence of hot electrons mean energy on the intensity changes qualitatively in relativistic interaction mode. This fact points at alternative mechanisms of electrons acceleration, which might be due to the production of extended area of subcritical plasma by the pre-pulse. Such mechanisms could be stimulated Raman scattering and three-plasmon instability [23], relativistic self-focusing [24] and stimulation of longitudinal waves of electron density (wake field electrons acceleration).

Stimulated Raman scattering and three-plasmon instability show intensity-threshold behavior and develop intensively in plasma area, where electrons concentration is $n_e \sim n_c/4$ (n_c – critical density of plasma). Both of these processes cause generation of $3/2\omega_0$ component in the spectrum of the reflected radiation. However, we have not observed radiation at $\sim$530 nm wavelength in our experiments.

Relativistic self-focusing of laser radiation in plasma with subcritical density develops only when radiation power P_1 exceeds self-focusing critical power [24] $P_{cr} = 17\frac{n_c}{n_e}$ GW. Maximum peak power of radiation in our experiment (300 GW) is well in excess of this value. When the pre-pulse amplitude is high, the spatial scale of plasma gradient is L$\sim$ 100-200 mkm [23] and becomes comparable with the laser radiation Rayleigh length (about 20 mkm). Diameter of the laser beam, which is formed during relativistic self-focusing, is defined by plasma density n_e [25] $d_{sf} = \frac{2\lambda}{\pi}\sqrt{\frac{n_c}{n_e}}$. Estimates show that at $\sim$10L distance from a target diameter of the focused beam d becomes of the order of d_{sf}. Closer to the target, beam diameter further decreases due to increase in the plasma density and converges to the current value $d_{sf}(n_e)$ [25]. Minimum of 0.5 mkm d_{sf} achieves when $n_e \sim n_c$, and intensity may increase up to 9x10^{19} W/cm^2 in this case. With high nanosecond contrast scale L was defined by picoseconds contrast and was about 0.1-1 mkm. Apparently, in this case relativistic self-focusing has not enough length to develop, and beam diameter collapse does not occur.

Wake-field laser-plasma electron acceleration is usually realized at pulse energies exceeding the ones in our experiments, and at intensities about 10^{18} – 10^{19} W/cm^2 [12]. Higher laser pulse energy is required to provide electron acceleration at longer distances. Estimations show that maximal energy, which electron can gain on the length equal to half Rayleigh length, is about 2.4 MeV at 15 mJ energy in our focusing conditions.

Thus, observed increase in the mean (and maximal) energy of electrons may be related to the relativistic self-focusing of radiation, as well as to laser-plasma electron acceleration. It should be noted that relativistic self focusing effect upon ions acceleration in plasma was observed recently in the work [26], and seemingly played

important role in many published studies, where subpicosecond and femtosecond laser radiation with intensity more than 10^{17} W/cm^2 was used. To get more insight into the physical origin of the observed phenomenon, it is, of course, necessary to perform numerical (PIC) simulations of interaction of relativistic laser radiation with long spatial gradient plasma.

Acknowledgements Authors are grateful to Dr. A.Paskhalov and Dr. N.Eremin for their help while conducting high energy x-ray quanta detection. Experiments were made using ILC MSU multi-user Ti:Sa facility. This work was supported by Russian Foundation for Basic Research (grant 07-02-00724a).

References

[1] P. Gibbon, R. Forster, Plasma Phys. Control. Fus., **38**, 769 (1996).
[2] A.A. Andreev, E.G. Gamaly, V.N. Novikov, A.N. Semakhin, V.T. Tikhonchuk, Proc. SPIE, **1800**, 86 (1992).
[3] A.A. Andreev *et al.*, Zh. Eksp. Teor. Fiz., **101** (1992).
[4] D.W. Forslund, J.M. Kindel, K. Lee, Phys. Rev. A, **11**, 679 (1975).
[5] D.W. Forslund, J.M. Kindel, K. Lee, Phys. Rev. Let., **39**, 284 (1977).
[6] F. Brunel, Phys. Rev. Let., **59**, 52 (1987).
[7] P. Gibbon, A.R. Bell, Phys. Rev. Let., **68**, 1535 (1992).
[8] S.C. Wilks, Phys. Fluids B, **5**, 2603 (1993).
[9] L.D. Landau, E.M. Lifshitz, Classical Theory of Fields, Butterworth-Heinemann, 4^{th} edition (1980).
[10] W.L. Kruer and K. Estabrook, Phys. Fluids,
textbf28, 430 (1985).
[11] T. Tajima, J.M. Dawson, Phys. Rev. Lett., **43**, 267 (1979).
[12] V. Malka, J. Faure *et al.*, Physics of Plasmas, *16*, 056703 (2009).
[13] Y.T. Li, J. Zhang, Z.M. Sheng, J. Zheng, Z.L. Chen, R. Kodama, T. Matsuoka, M. Tampo, K.A. Tanaka, T. Tsutsumi, T. Yabuuchi, Phys. Rev. E, **69**, 036405 (2004).
[14] V.V. Bolshakov, A.A. Vorobyev *et al.*, Applied Physics, **1**, 18 (2009).
[15] D.M. Golishnikov, V.M Gordienko, P.M. Mikheev *et al.*, Laser Phys., **11**, 1205 (2001).
[16] Gordienko V.M., Makarov I.A., Rakov E.V., Savel'ev A.B., Quantum Electronics, **35**(6), 487 (2005).
[17] S.A. Akhmanov, S.Yu. Nikitin, Physical Optics, Oxford University Press, USA (1997).
[18] Xu Hui, Sheng Zheng-Ming, Zhang Jie, Yu M.Y., Phys. of Plasmas, 13, 123301 (2006).
[19] D. Von der Linde, K. Sokolowski-Tinten, J. Bialkowski, Appl. Surf. Scien., **109**, 1 (1997).
[20] B.C. Stuart, M.D. Feit, S. Hermanv *et al.*, Phys. Rev. B, 53, 1749 (1996).
[21] D.F. Cai, Y.Q. Gu, Z.J. Zheng, W.M. Zhou *et al.*, Phys. Rev. E, **70**, 066410 (2004).
[22] F.N. Beg, A.R. Bell, A.E. Dangor *et al.*, Phys. Plasmas **4**, 447 (1997).
[23] L. Veisz, W. Theobald, T. Feurer *et al.*, Phys. of Plasmas, **9**, 3197 (2002).
[24] A.B. Borisov, A.V. Borovskiy, O.B. Shiryaev *et al.*, Phys. Rev. A, **45**, 5830 (1992).
[25] J. Davis, A.B. Borisov, and C. Rhodes, Phys. Rev. E, **70**, 066406 (2004).
[26] A.Ya. Faenov, A.I. Magunov, S.A. Pikuz, I.Yu. Skobelev *et al.*, Journal of Experimental and Theoretical Physics, **84**, 308 (2006).

